



Toward a physics design for NDCX-II, an ion accelerator for warm dense matter and HIF target physics studies

A. Friedman^{a,e,*}, J.J. Barnard^{a,e}, R.J. Briggs^{b,e}, R.C. Davidson^{c,e}, M. Dorf^{c,e}, D.P. Grote^{a,e}, E. Henestroza^{b,e}, E.P. Lee^{b,e}, M.A. Leitner^{b,e}, B.G. Logan^{b,e}, A.B. Sefkow^{c,e}, W.M. Sharp^{a,e}, W.L. Waldron^{b,e}, D.R. Welch^d, S.S. Yu^{b,e}

^a Lawrence Livermore National Laboratory, Livermore, CA, USA

^b Lawrence Berkeley National Laboratory, Berkeley, CA, USA

^c Princeton Plasma Physics Laboratory, Princeton, NJ, USA

^d Voss Scientific, Albuquerque, NM, USA

^e Heavy Ion Fusion Science Virtual National Laboratory, USA

ARTICLE INFO

Available online 5 April 2009

Keywords:

Accelerator
Fusion
Heavy-ion
Induction
Simulation
Particle-in-cell
Plasma
Beam

ABSTRACT

The Heavy Ion Fusion Science Virtual National Laboratory (HIFS-VNL), a collaboration of LBNL, LLNL, and PPPL, has achieved 60-fold pulse compression of ion beams on the Neutralized Drift Compression eXperiment (NDCX) at LBNL. In NDCX, a ramped voltage pulse from an induction cell imparts a velocity “tilt” to the beam; the beam’s tail then catches up with its head in a plasma environment that provides neutralization. The HIFS-VNL’s mission is to carry out studies of warm dense matter (WDM) physics using ion beams as the energy source; an emerging thrust is basic target physics for heavy ion-driven inertial fusion energy (IFE). These goals require an improved platform, labeled NDCX-II. Development of NDCX-II at modest cost was recently enabled by the availability of induction cells and associated hardware from the decommissioned advanced test accelerator (ATA) facility at LLNL. Our initial physics design concept accelerates a ~ 30 nC pulse of Li^+ ions to ~ 3 MeV, then compresses it to ~ 1 ns while focusing it onto a mm-scale spot. It uses the ATA cells themselves (with waveforms shaped by passive circuits) to impart the final velocity tilt; smart pulsers provide small corrections. The ATA accelerated electrons; acceleration of non-relativistic ions involves more complex beam dynamics both transversely and longitudinally. We are using an interactive one-dimensional kinetic simulation model and multidimensional Warp-code simulations to develop the NDCX-II accelerator section. Both LSP and Warp codes are being applied to the beam dynamics in the neutralized drift and final focus regions, and the plasma injection process. The status of this effort is described.

© 2009 Elsevier B.V. All rights reserved.

1. Introduction

The Heavy Ion Fusion Science Virtual National Laboratory (HIFS-VNL), a collaboration of Lawrence Berkeley National Laboratory, Lawrence Livermore National Laboratory, and Princeton Plasma Physics Laboratory, is applying intense ion beams as drivers for basic studies of warm dense matter (WDM) physics in uniformly heated foils driven by ions near the Bragg peak energy, and is studying their ultimate application for inertial fusion energy (IFE). For an overview of this effort, see Ref. [1]; more information can be found in Ref. [2]. An emerging emphasis is on

* Corresponding author at. Lawrence Livermore National Laboratory, Livermore, CA, USA. LBNL, MS 47R0112, One Cyclotron Road, Berkeley, CA 94720, USA. Tel.: +1 510 486 5592.

E-mail address: af@llnl.gov (A. Friedman).

the novel properties of ion direct drive for inertial fusion energy [3]. On the Neutralized Drift Compression eXperiment (NDCX) at LBNL, a velocity “tilt” is imparted to the beam as it traverses an induction gap by a ramped voltage pulse; the beam’s tail then catches up with its head in a plasma environment that provides needed neutralization. Using this technique, compression factors of 60 or greater have been achieved [4,5]. These studies are employing K^+ ions at 350 keV and ~ 25 mA. Greater uniformity of energy deposition would be obtained by using ions that impinge on the target foil at an energy slightly above the Bragg peak, then slow in the target and exit at an energy slightly below that peak; this requires an improved facility, NDCX-II.

We have developed the basis for an attractive physics design for NDCX-II. Our goal is a machine concept capable of meeting the needs of the WDM research program described above and, after straightforward extension, of supporting a rich set of ion-beam-driven target experiments to explore fundamental aspects of ion

direct drive. Section 2 briefly outlines the options considered. Section 3 describes the elements of the evolving NDCX-II physics design as developed using a one-dimensional (1-D) discrete-particle model. Section 4 describes multidimensional simulation studies that validate and expand on the 1-D work [6], and that examine the physics of plasma injection and beam neutralization in NDCX-II. Finally, Section 5 discusses both planned and possible future work in this area.

2. Options for NDCX-II

A study [7] of ion beam drivers for creating WDM conditions explored several approaches to accelerate and compress 30 nC of Li^+ ions to 2.8 MeV or more. Three options were considered, all beginning with an injector that produces a 100 keV beam: (a) a 3-m electrostatic column (with 10 kV/cm gradient); (b) a sequence of pulse-line ion accelerator (PLIA) sections, running in the “snowplow” mode; and (c) an induction accelerator using cells from the decommissioned advanced test accelerator (ATA) at LLNL. All three concepts appeared feasible, but the maturity of the induction approach and the existence of much of the hardware has led us to select that approach as our baseline. Research into the PLIA approach continues in the HIFS-VNL [9–11] and at the Chinese University of Hong Kong (CUHK) [12]; a PLIA might serve as a front-end upgrade, or as an “afterburner” for higher energy.

While several approaches to generating an initial beam with a high line charge density are possible, we plan to extract a long, high-current pulse from a diode at relatively high energy, and then pass the beam through a decelerating field to compress it, in an “accel–decel” configuration. To understand this, consider a lossless steady injection: the current is constant along the axis, so the slower downstream beam has an increased line-charge density. The low-energy beam bunch is directed into a solenoid and matched into a Brillouin flow. The Brillouin equilibrium is independent of the energy if the relationship among the beam size (a), solenoid magnetic field strength (B), and line charge density (λ) is such that $(Ba)^2$ is proportional to λ . Such an “accel–decel” system serves as the front end of our physics design

concept for NDCX-II. To explore this type of injector, an experiment has been formulated [8] in which we would extract a $\sim 1 \mu\text{s}$, 100 mA K^+ beam at 160 keV, and decelerate it to 55 keV ($\lambda \sim 0.2 \mu\text{C/m}$).

3. Elements of physics design

The arrangement of induction cells and applied accelerating waveforms that we propose is novel, but the system is based on well-established technologies. It takes full advantage of the available ATA ferromagnetic cells and Blumleins. The system is compact, and relies heavily on passive circuit elements to provide the requisite waveform shaping. The adaptation from ATA, which accelerated electrons, has been nontrivial, because of the need to aggressively compress the ion pulse from its initial ~ 500 ns duration to ~ 1 ns, as required for the WDM physics mission. The applied waveforms must simultaneously impose a head-to-tail velocity tilt, compensate for the beam space charge, and accelerate the beam.

Using a 1-D particle-in-cell simulation code designed for this purpose, we developed an acceleration schedule employing 30 ATA cells (20 driven by the ATA Blumleins, plus 10 with lower-voltage sources). To reduce the axial extent of the gap fringe fields, the 6.7-cm radius of the ATA beam pipe is reduced to 4.0 cm. This system accelerates a Li^+ beam (100 keV as injected, with a 67 mA flat-top) to 3.5 MeV at ~ 2 A, and imparts an 8% tilt. After neutralized drift compression, about 75% of the 30 nC beam charge crosses the focal plane in a 1-ns window, with a minimal pre-pulse. The current of the compressed beam (averaged over that window) is ~ 23 A, with a peak (averaged over a 0.1-ns window) of ~ 32 A and a full-width at half maximum of ~ 1 ns.

A novel two-part strategy is employed to accelerate and compress the beam. In (roughly) the first half of the lattice, the pulse is rapidly compressed via “non-neutral drift compression.” The beam transit time through an acceleration gap (including its axially extended fringe field) must be less than 70 ns for a high-voltage (up to ~ 200 kV) ATA Blumlein to be used as the pulser. Custom pulsers at lower voltage are required for longer pulses; to

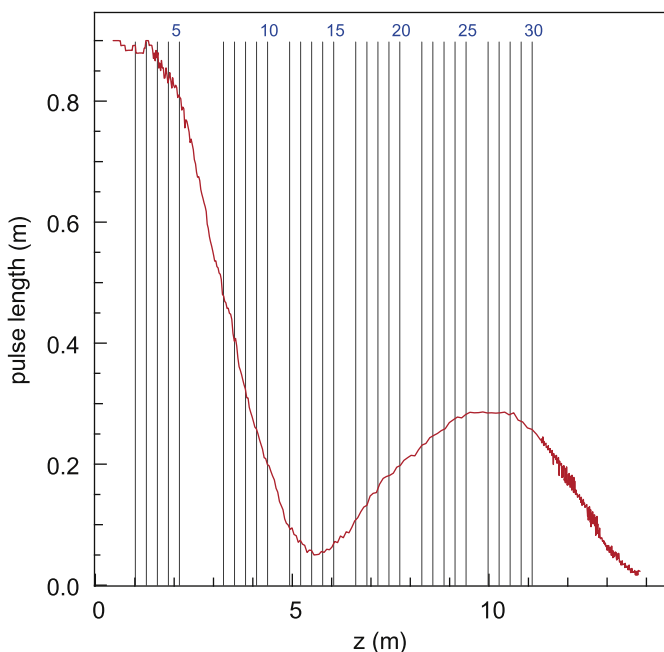


Fig. 1. Pulse length vs. axial coordinate z . Numbers label the accelerating gaps.

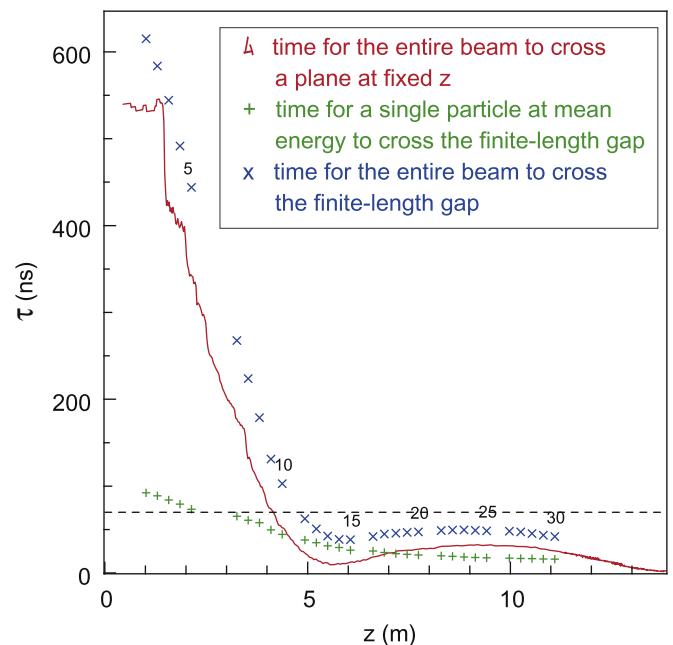


Fig. 2. Pulse duration vs. z ; the key measure is the time for the entire beam to traverse a gap’s extended fringe field from entrance to exit.

minimize the number of these, we use the volt-seconds of the first two cell blocks to impose a velocity tilt, with space between tilt cells for drift compression and longitudinal control. To avoid short-wavelength density irregularities, we choose the tilt-cell fields to maintain, insofar as possible, a linear velocity variation

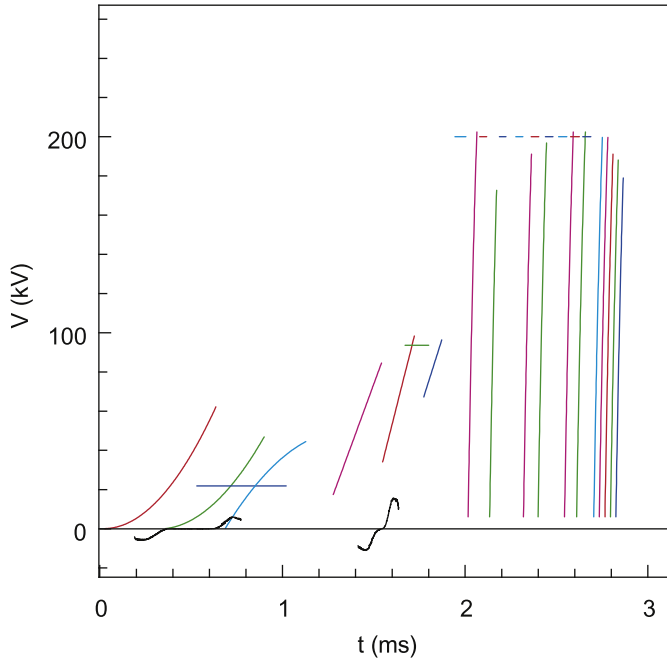


Fig. 3. Waveforms for accelerating gaps as developed using 1-D simulations.

and a smooth density profile. We obtain the desired waveforms using a least-squares optimization that penalizes both nonlinearity and nonuniformity.

In the second half of the lattice, the beam is allowed to lengthen as it is accelerated, with only enough ramped pulses added to keep the duration under 70 ns. The initial compression is slowed by the increasing space-charge field; after the beam passes through a longitudinal waist, it begins to lengthen as a consequence of acceleration and space charge. Since the beam at the waist is shorter than the longitudinal extent of the gap fields, those fields cannot prevent this “bounce;” however, as the length increases, tilt cells can keep the beam duration from exceeding 70 ns. We find that two tilt cells in each block of five suffice. The modularity of these blocks is an attractive feature, since more can be added if a higher final kinetic energy is desired. A final block with five ramped pulses applies the tilt for neutralized drift compression onto the target; this is another attractive feature, since no high-voltage “tilt core” is required. Fig. 1 shows the evolution of the beam length, while Fig. 2 shows the evolution of the pulse duration.

All the waveforms in this acceleration schedule, except for the longitudinal-control fields or “ears” applied in the first two blocks, are simple enough to be formed with passive circuits in the “compensation boxes” that are attached to the ATA cells. For the case discussed here, all the tilt-cell waveforms in the final four cell blocks have been generated by solving appropriate circuit equations, producing the nearly “triangular” (linearly rising from zero) pulses seen in Fig. 3. Similar circuits are being studied to form the tilt waveforms in the first two blocks. The low-voltage highly shaped “ear” waveforms may require programmable circuits like those developed by First Point Scientific. Fig. 4 shows the evolution of the beam phase space

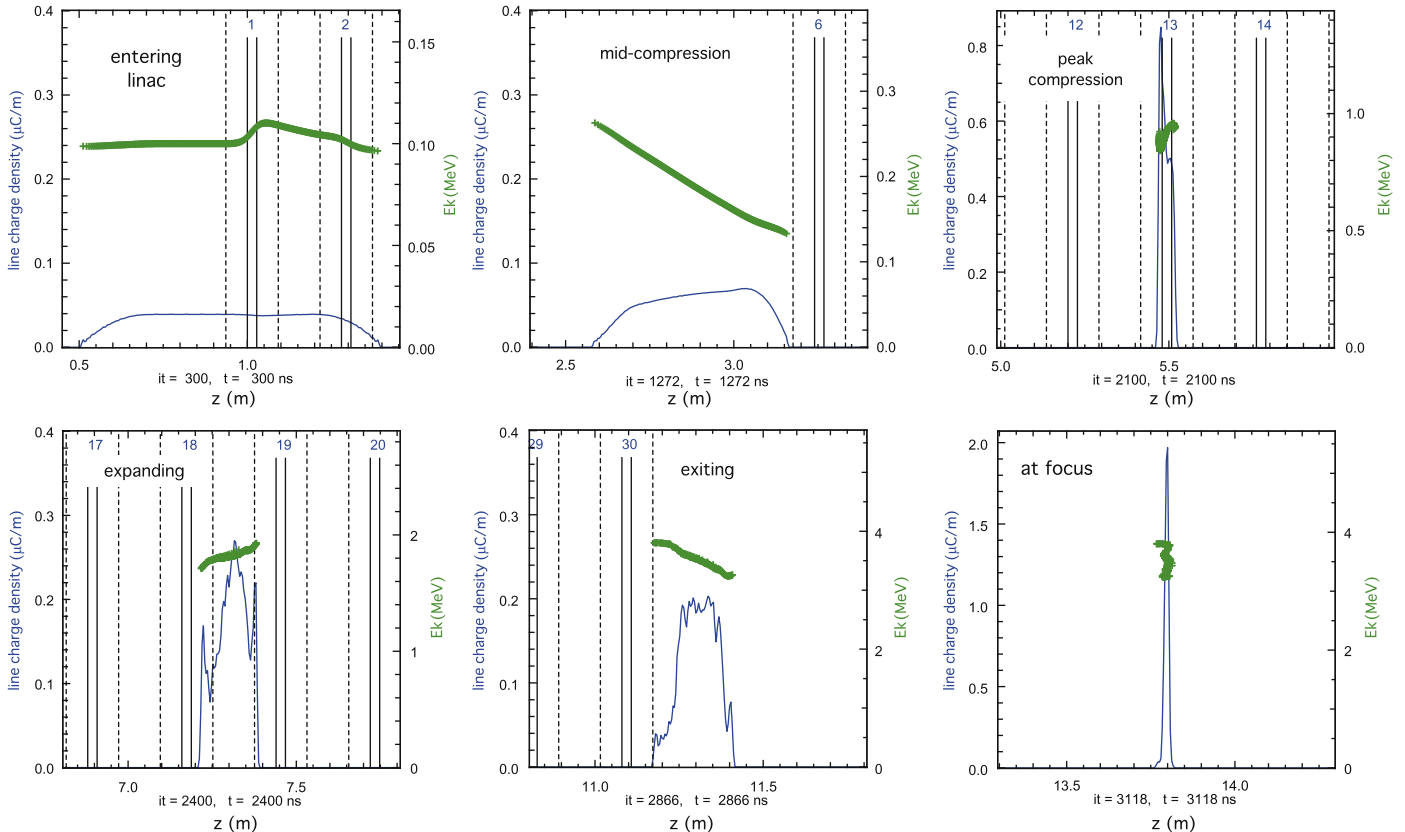


Fig. 4. Snapshots from 1-D code at selected times: longitudinal phase space of energy vs. z position (right ordinate scale, individual markers); and λ (averaged over ~ 4 mm) (left ordinate scale, thin trace).

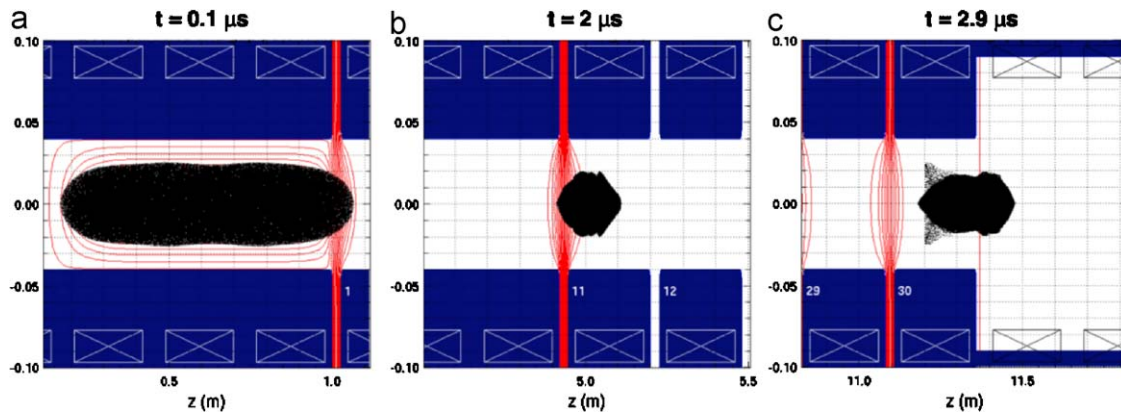


Fig. 5. Views of beam in (x, z) projection at selected times, as simulated using Warp. The inductive accelerating field is treated, to good approximation, as electrostatic, so contour lines denote equipotentials.

and line-charge-density profile; its final panel shows the beam when its centroid is at the “best longitudinal focus” plane. This plane is estimated by an RMS measure [13] and then refined by explicitly finding that plane through which the most current flows in an optimal 1-ns window.

4. Multidimensional simulation studies

While the 1-D results described above are encouraging, that model necessarily omits radial variation of the acceleration and space charge fields, as well as the physics of transverse confinement and focusing. The 1-D model is validated by initial axisymmetric (r, z) simulations using the Warp code (the name derives from the code’s ability to simulate bent beam-lines using a “warped” computational grid). When we use the acceleration fields shown in Fig. 3 and an initial Warp beam with the same line-charge, energy, and longitudinal profile, no particles are lost and the final energy and pulse duration are similar to the 1-D results of Fig. 4. As shown in Fig. 5, the transverse dynamics is well behaved although there is some envelope mismatch; the normalized transverse emittance grows from 0.9 to 1.2 mm-mr in the accelerator. Fig. 6 shows snapshots taken at the same time from 1-D and Warp runs, for similar conditions; the gross beam characteristics, and the energy, are quite similar, but the details of the phase space and line-charge density profile differ. Some fine-tuning of the parameters of the 1-D model (e.g., the scale-length for transverse field fall-off used in the Poisson equation that is solved to obtain the space-charge field [14]) might improve the agreement, but in any event final adjustments of waveforms will be done in Warp. This early Warp run yields somewhat poorer compression than was obtained in 1-D, with a peak current about 30% lower. Adjustments of the strengths of the 2–3 T confining solenoids in the accelerator and the final 8–15 T focusing solenoid are ongoing.

Efforts are in progress to use Warp to simulate the NDCX-II beam from the source to the target plane. These simulations are more challenging than the run described above (which was initiated with a uniform-energy beam) because the ion beam already has a significant energy variation by the time it reaches the first gap, due to both transit-time effects in the diode and the longitudinal space-charge field. To remove most of this initial energy nonuniformity, we use an ear cell immediately after injection. Initializing the 1-D code with a beam containing an idealized energy variation, we have developed an acceleration schedule that produces a beam with nearly the same final parameters as those found for the initially monoenergetic beam, but with a small fraction of straggling ions at lower energies. Early

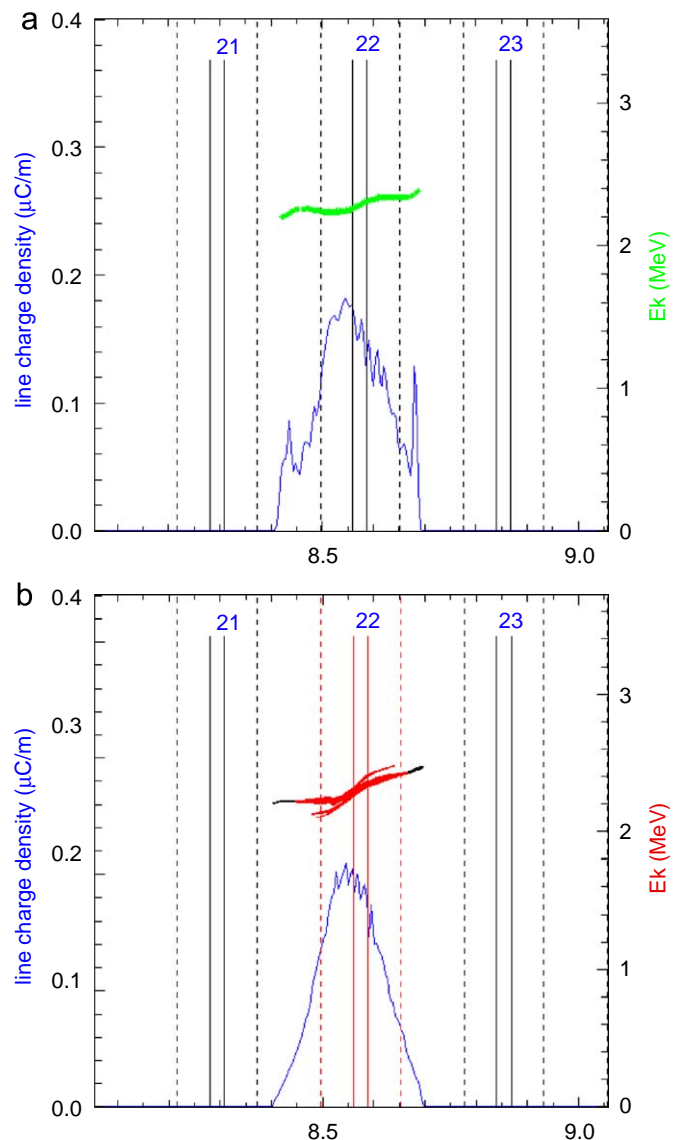


Fig. 6. (E_k, z) phase space and line-charge density at $2.58 \mu\text{s}$ from (a) 1-D code run and (b) Warp run.

Warp results with this new schedule give a beam with the correct final energy and a somewhat smaller head-to-tail velocity tilt; we are presently working to improve this case.

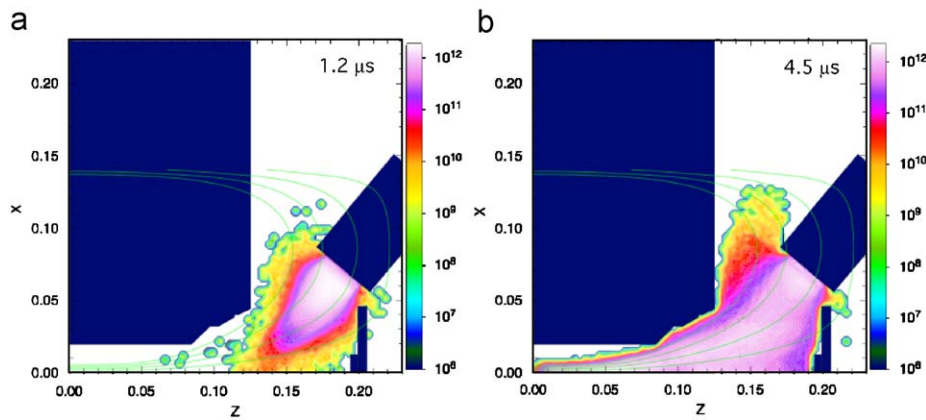


Fig. 7. Frames from a Warp simulation of plasma injection at (a) 1.2 μs and (b) 4.5 μs .

As the beam leaves the accelerator it is neutralized and allowed to drift-compress until it passes through a final strong solenoid and is focused onto the target. Extensive calculations of both the beam dynamics of this process and the injection of plasma have been carried out using the large scale plasma (LSP) code; for an overview and a description of an integrated calculation for NDCX-I, see Ref. [15]. The reference also details the “Lee” accelerating-gap field model employed in our 1-D studies; we use a single-term approximation because the fringing length is much greater than the physical gap length. Warp is also being used for neutralized-beam and plasma injection studies relevant to both NDCX-I and NDCX-II. As an example, Fig. 7 shows a snapshot from a simulation of plasma injection by the cathodic arc plasma sources (CAPS) in NDCX-I; colors denote the plasma density.

5. Future directions

Our 1-D simulations suggest that the beam is insensitive to waveform details after the initial compression. However, tolerances for waveform timing and voltage need be developed with two-dimensional Warp studies. Three-dimensional studies will develop steering techniques and establish tolerances for the alignment and field strength of solenoids. We will use simulations and analysis to develop an optimized final focusing system, accounting for the dependence of the size and profile of the focal spot upon the velocity tilt, focusing angle, chromatic aberration, and properties of the neutralizing background plasma [16]. The ability of time-dependent focusing to correct for chromatic effects [17] in NDCX-II will be quantified, and a practical design worked out. We will explore various means of plasma injection and control for neutralized compression and focusing; alternatives to the CAPS may prove superior.

While to date we have concentrated on an initial NDCX-II configuration aimed at WDM studies, a smaller amount of work has considered the modifications necessary to produce higher kinetic energies, multiple pulses, and/or longer pulses with

ramped energy, to study energy coupling and hydrodynamic stability in ion direct drive. NDCX-II promises to be a flexible facility capable of supporting a wide range of experiments.

Acknowledgments

This work was performed under the auspices of the U.S. DOE by LLNL under Contract DE-AC52-07NA27344, by LBNL under Contract DE-AC02-05CH11231, and by PPPL under Contract DE-AC02-76CH03073.

References

- [1] B.G. Logan, et al., Nucl. Instr. and Meth. A 577 (2007) 1.
- [2] Y. Oguri (Ed.), Proceedings of the 17th International Symposium on Heavy Ion Inertial Fusion (HIF2008), Tokyo, August 4–9, 2008, hereafter referred to as these Proceedings.
- [3] B.G. Logan, et al., these Proceedings.
- [4] J.E. Coleman, et al., Proceedings of the 2007 Particle Accelerator Conference (<http://accelconf.web.cern.ch/AccelConf/>).
- [5] P.A. Seidl, these Proceedings.
- [6] W.M. Sharp, et al., these Proceedings.
- [7] J.J. Barnard (Ed.), Summary and Proceedings of the Workshop on Accelerator Driven Warm Dense Matter Physics, Pleasanton, CA, February 2006 (http://hifnews.lbl.gov/HIFNewsNo3_06.pdf) and (<http://hifweb.lbl.gov/public/AcceleratorWDM/proceedings/>).
- [8] E. Henestroza, et al., Proceedings of the 2005 Particle Accelerator Conference (<http://accelconf.web.cern.ch/AccelConf/>).
- [9] R.J. Briggs, Phys. Rev. ST Accel. Beams 9 (2006) 060401.
- [10] A. Friedman, et al., Proceedings of the 2007 Particle Accelerator Conference (<http://accelconf.web.cern.ch/AccelConf/>).
- [11] W.L. Waldron, et al., Proceedings of the 2007 Particle Accelerator Conference (<http://accelconf.web.cern.ch/AccelConf/>).
- [12] C.Y. Ling, et al., these Proceedings.
- [13] A. Friedman, Some kinematic aspects of neutralized drift compression, LLNL Research Note LLNL-TR-402447, March 18, 2008.
- [14] J.J. Barnard, et al., Proceedings of the 1993 Particle Accelerator Conference (<http://accelconf.web.cern.ch/AccelConf/>).
- [15] D.R. Welch, et al., Phys. Rev. ST Accel. Beams 11 (2008) 064701.
- [16] J. J. Barnard, et al., Proceedings of the 2005 Particle Accelerator Conference (<http://accelconf.web.cern.ch/AccelConf/>).
- [17] E.P. Lee, Proceedings of the IFE Science and Technology Strategic Planning Workshop, San Ramon, CA, April 24–27, 2007, Part 5, pp. 109–124 (<http://ifeworkshop.llnl.gov/proceedings.html>).